Origami Folding: A Structural Engineering Approach

Mark Schenk and Simon D. Guest

March 8, 2011

Abstract

In this paper we present a novel engineering application of Origami, using it for both the flexibility and the rigidity the folding patterns provide. The proposed Folded Textured Sheets have several interesting mechanical properties. The folding patterns are modelled as a pin-jointed framework, which allows the use of established structural engineering methods to gain insight into the kinematics of the folded sheet. The kinematic analysis can be naturally developed into a stiffness matrix approach; by studying its softest eigenmodes, important deformations of a partially folded sheet can be found, which aids in the understanding of Origami sheets for engineering applications.

1 Introduction

For structural engineers, Origami has proven to be a rich source of inspiration, and it has found its way into a wide range of structural applications. This paper aims to extend this range and introduces a novel engineering application of Origami: *Folded Textured Sheets*.

Existing applications of Origami in engineering can broadly be categorized into three areas. Firstly, many deployable structures take inspiration from, or are directly derived from, Origami folding. Examples are diverse and range from wrapping solar sails [Guest and Pellegrino 92] to medical stents [Kuribayashi et al. 06] and emergency shelters [Temmerman 07]. Alternatively, folding is used to achieve an increase in stiffness at minimal expense of weight, for example in the design of light-weight sandwich panel cores for aircraft fuselages [*e.g.* Heimbs et al. 07]. In architecture the principle is also applied, ranging from straightforward folded plate roofs to more complicated designs that unite an increase in strength with aesthetic appeal [Engel 68]. Thirdly, Origami patterns have been used to design shock absorbing devices, such as car crash boxes with Origami-inspired

patterns that induce higher local buckling modes [Weina and You 10], and packaging materials [Basily and Elsayed 04].

In contrast to existing engineering applications, the Folded Textured Sheets introduced in this paper use Origami for a different, and slightly paradoxical, purpose: both for the flexibility and the stiffness that it provides. The Origami folding patterns enable the sheets to deform easily into some deformation modes, whilst remaining stiff in others. This anisotropy in deformation modes is for example of interest for applications in morphing structures; these types of structures are capable of changing their shape to accommodate new requirements, whilst maintaining a continuous external surface.

1.1 Outline

Section 2 introduces two example Folded Textured Sheets, the Eggbox and Miura sheet, and will highlight some of their mechanical properties of interest. Section 3 describes the mechanical model in detail, interleaved with results for the two example sheets.

2 Folded Textured Sheets

The Folded Textured Sheets form part of ongoing research into the properties and applications of textured sheets. By introducing a 'local' texture (such as corrugations, dimples, folds, etc.) to otherwise isotropic thin-walled sheets, the 'global' mechanical properties of the sheets can be favourably modified. The 'local' texture has no clearly defined scale, but lies somewhere between the material and the structural level and in effect forms a microstructure. The texture patterns in Folded Textured Sheets are *inspired* by Origami folding, as the resulting sheets need not necessarily be developable. The texture consists of distinct fold lines, and it is therefore better to speak of polygonal faceted surfaces. See Figure 1 for the two example sheets used in this paper: the *Eggbox* and *Miura* sheet.

The first obvious property of the folded sheets is their ability to undergo relatively large deformations, by virtue of the folds opening and closing. Moreover, the fold patterns enable the sheets to locally expand and contract — and thereby change their global Gaussian curvature — without any stretching at material level. Gaussian curvature is an intrinsic measure of the curvature at a point on a surface, which remains invariant when bending, but not stretching the surface [Huffman 76]. Our interest lies with the macroscopic behaviour of the sheets, and we therefore consider the 'global' Gaussian curvature of an equivalent mid-surface of the folded sheet. Both the Eggbox and Miura sheets are initially flat, and thus have a zero global

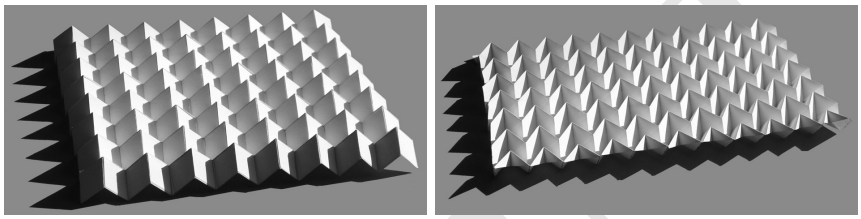

(a) overview of folded textured sheets

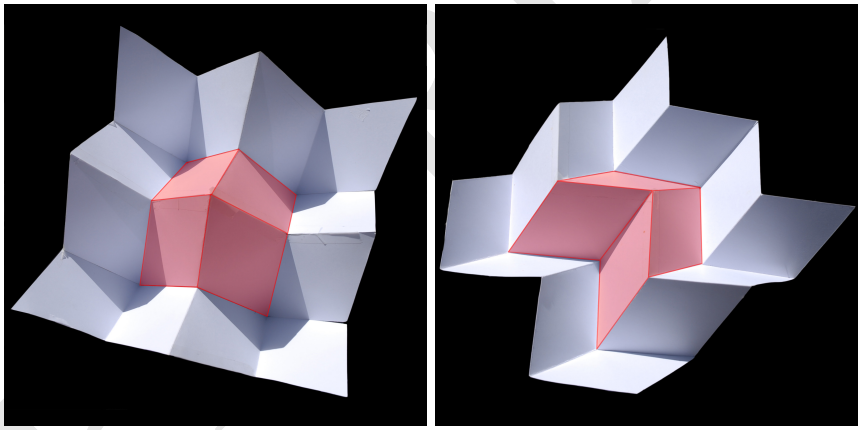

(b) close-up of unit cells

Figure 1: photographs of the Eggbox (left) and the Miura sheet (right). The models are made of standard printing paper, and the parallelograms in both sheets have sides of 15mm and an acute angle of 60°. The Miura sheet is folded from a single flat sheet of paper; the Eggbox sheet, in contrast, is made by gluing together strips of paper, and has (equal and opposite) angular defects at its apices and saddle points.

Gaussian curvature. Now, unlike conventional sheets, both folded textured sheets can easily be twisted into a saddle-shaped configuration which has a globally negative Gaussian curvature — see Figure 2(a) and Figure 3(a).

The sheets' most intriguing property, however, relates to their Poisson's ratio. Both sheets have a single in-plane mechanism whereby the facets do not bend and the folds behave as hinges; by contrast, facet bending is necessary for the out-of-plane deformations. As shown in Figure 2(b) and Figure 3(b), the Eggbox and the Miura sheet respectively have a positive and a negative Poisson's ratio in their planar deformation mode. A negative Poisson's ratio is fairly uncommon, but can for instance be found in foams with a reentrant microstructure [Lakes 87]. Conventionally, materials with a positive Poisson's ratio will deform anticlastically under bending (*i.e.*, into a saddle-shape) and materials with a negative Poisson's ratio will deform synclastically into a spherical shape. As illustrated in Figure 2(c) and Figure 3(c), however, both folded textured sheets behave exactly opposite to what is conventionally expected, and their Poisson's ratio is of opposite sign for in-plane stretching and out-of-plane bending. This remarkable mechanical behaviour has only been described theoretically for auxetic composite laminates [Lim 07] and specially machined chiral auxetics [Alderson et al. 10], but is here observed in textured sheets made of conventional materials.

2.1 Engineering Applications

Our interest in the Folded Textured Sheets is diverse. Firstly, they can undergo large global deformations as a result of the opening and closing of the folds. Furthermore, these folds provide flexibility in certain deformation modes, whilst still providing an increased bending stiffness. This combination of flexibility and rigidity is of interest in morphing structures, such as the skin of morphing aircraft wings [Thill et al. 08].

Another interesting property of the folded sheets is their ability to change their global Gaussian curvature, without stretching at material level. This is of interest in architectural applications, where it may be used as cladding material for doubly-curved surfaces, or, at a larger scale, as flexible façades. Furthermore, the use of the sheets as reusable doubly-curved concrete formwork is being explored; work is still ongoing to determine the range of surface curvatures that these sheets can attain.

Applications for the remarkable behaviour of the oppositely signed Poisson's ratios under bending and stretching are still being sought. Nevertheless, the folded sheets add a new category to the field of auxetic materials.

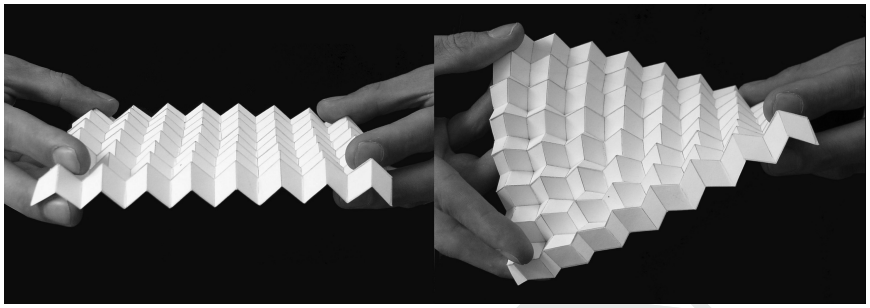

(a)

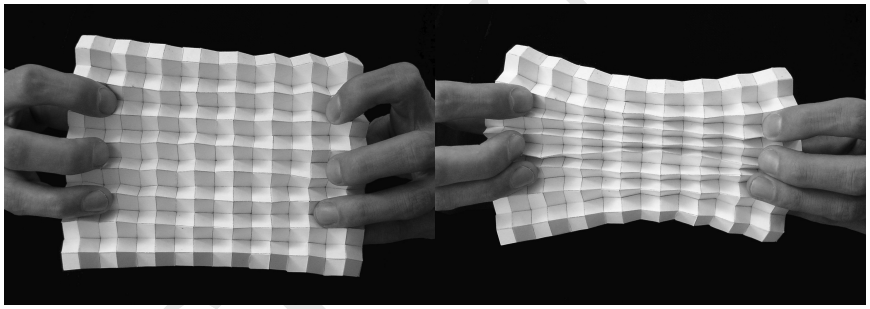

(b)

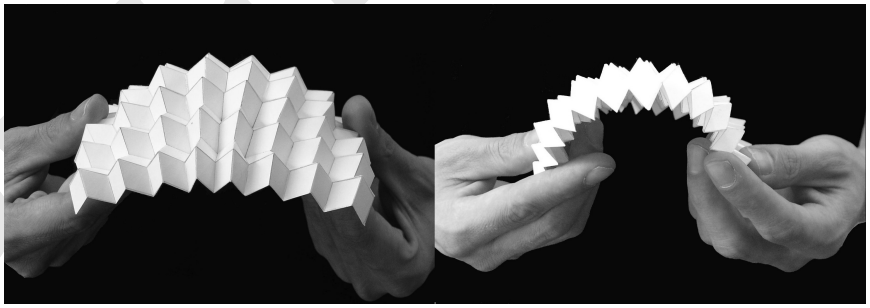

(c)

Figure 2: mechanical behaviour of the Eggbox sheet. Firstly, it can change its global Gaussian curvature by twisting into a saddle-shaped configuration (a). Secondly, the Eggbox sheet displays a positive Poisson's ratio under extension (b), but deforms either into a cylindrical or a spherical shape under bending (c). The spherical shape is conventionally seen in materials with a negative Poisson's ratio.

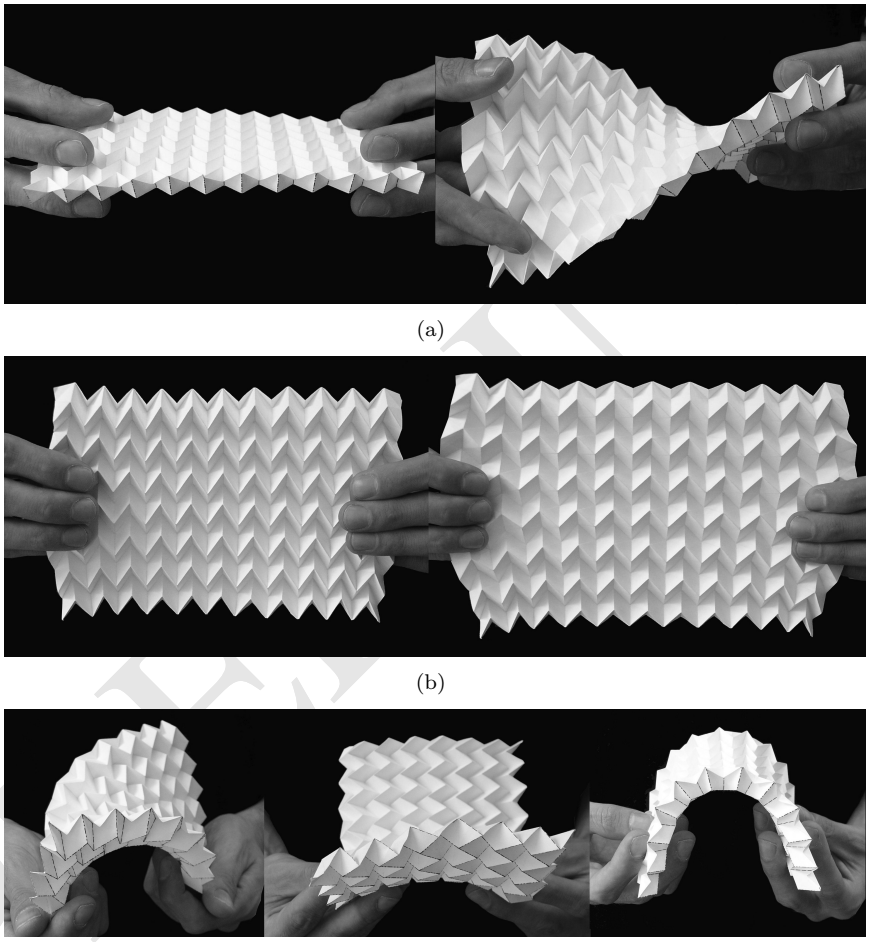

Figure 3: mechanical behaviour of the Miura sheet; it can be twisted into a saddle-shaped configuration with a negative global Gaussian curvature (a). Secondly, the Miura sheet behaves as an auxetic material (negative Poisson's ratio) in planar deformation (b), but it assumes a saddle-shaped configuration under bending (c), which is typical behaviour for materials with a positive Poisson's ratio.

3 Mechanical Modelling Method

Available mechanical modelling methods for Origami folding broadly cover Rigid Origami simulators [Tachi 06, Balkcom 04] or methods describing paper as thin shells using Finite Elements. Our purpose is not to formulate an alternative method to describe rigid origami, as we aim to obtain different information. Neither do we wish to use Finite Element Modelling, since we are not interested in the minutiae of the stress distributions, but rather the effect of the introduced geometry on the global properties of the sheet. The salient behaviour straddles kinematics and stiffness: there are dominant mechanisms, but they have a non-zero stiffness. Our method needs to cover this behaviour. It should also not be limited to rigid origami as the out-of-plane kinematics of the sheets involves bending of the facets.

Our approach is based on modelling the partially folded state of a folded pattern as a pin-jointed truss framework. Each vertex in the folded sheet is represented by a pin-joint, and every fold line by a bar element. Additionally, the facets are triangulated to avoid trivial internal mechanisms, as well as provide a first-order approximation to bending of the facets — see Figure 4.

Although the use of a pin-jointed bar framework to represent Origami folding has been hinted at on several occasions [*e.g.*, Tachi 06, Watanabe and Kawaguchi 06], it has not been fully introduced into the Origami literature. The method provides useful insights into the mechanical properties of a partially folded Origami sheet, and has the benefit of an established and rich background literature.

3.1 Governing Equations

The analysis of pin-jointed frameworks is well-established in structural mechanics. Its mechanical properties are described by three linearized equations: equilibrium, compatibility and material properties.

$$\mathbf{At} = \mathbf{f} \tag{1}$$

$$\mathbf{Cd} = \mathbf{e} \tag{2}$$

$$\mathbf{Ge} = \mathbf{t} \tag{3}$$

where $\mathbf{A}$ is the *equilibrium* matrix, which relates the internal bar tensions $\mathbf{t}$ to the applied nodal forces $\mathbf{f}$; the *compatibility* matrix $\mathbf{C}$ relates the nodal displacements $\mathbf{d}$ to the bar extensions $\mathbf{e}$ and the material equation introduces the axial bar stiffnesses along the diagonal of $\mathbf{G}$. It can be shown through a straightforward virtual work argument that $\mathbf{C} = \mathbf{A}^T$, the static-kinematic duality.

3.2 Kinematic Analysis

The linear-elastic behaviour of the truss framework can now be described, by analysing the vector subspaces of the equilibrium and compatiblity matrices [Pellegrino and Calladine 86]. Of main interest in our case is the nullspace of the compatibility matrix, as it provides nodal displacements that — to first order — have no bar elongations: internal mechanisms.

$$\mathbf{Cd} = \mathbf{0}$$

These mechanisms may either be finite or infinitesimal, but in general the information from the nullspace analysis alone does not suffice to establish the difference. First-order infinitesimal mechanisms can be stabilised by states of self-stress, and a full tangent stiffness matrix would have to be formulated to take into account any geometric stiffness resulting from reorientation of the members.

In the case of the folded textured sheets, the nullspace of the conventional compatibility matrix does not provide much useful information: the triangulated facets can easily 'bend', which is reflected by an equivalent number of trivial internal mechanisms. The solution is to introduce additional contraints. The compatibility matrix can be reformulated as the Jacobian of the quadratic bar length constraints, with respect to the nodal coordinates. This parallel can be used to introduce additional equality constraints to the bar framework. In our case we add a constraint on the dihedral angle between two adjoining facets.

The angular constraint F is set up in terms of the dihedral fold angle θ between two facets. Using vector analysis, the angle between two facets can be described in terms of cross and inner products of the nodal coordinates $\mathbf{p}$ of the two facets (see Figure 5):

$$F = \sin(\theta) = \sin(\theta(\mathbf{p})) = \dots \tag{4}$$

and the Jacobian becomes

$$J = \frac{1}{\cos(\theta)} \sum \frac{\partial F}{\partial p_i} dp_i = d\theta \tag{5}$$

The Jacobian of additional constraints $\mathbf{J}$ can now be concatenated with the existing compatibility matrix

$$\begin{bmatrix} \mathbf{C} \\ \mathbf{J} \end{bmatrix} \mathbf{d} = \begin{bmatrix} \mathbf{e} \\ d\theta \end{bmatrix} \tag{6}$$

and the nullspace of this set of equations produces the nodal displacements $\mathbf{d}$ that do not extend the bars, as well as not violate the angular constraints. In effect, we have formulated a rigid origami simulator — no bending or

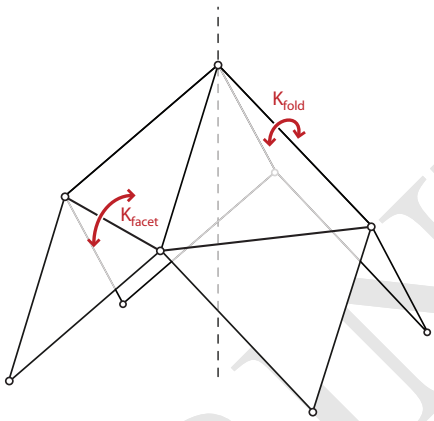

Figure 4: Unit cell of the Eggbox sheet, illustrating the pin-jointed bar framework model used to model the folded textured sheets. The facets have been triangulated, to avoid trivial mechanisms and provide a first-order approximation for the bending of the facets. Bending stiffness has been added to the facets and fold lines, K_{facet} and K_{fold} respectively.

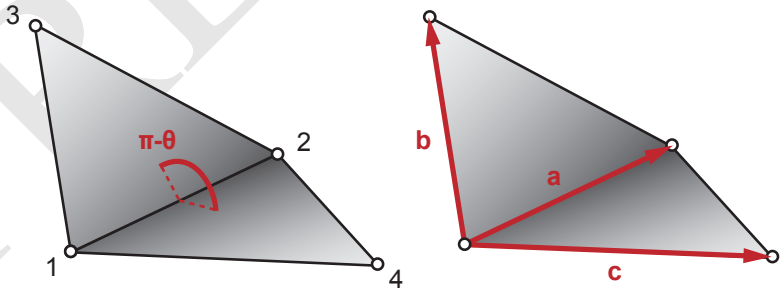

Figure 5: The dihedral fold angle θ can be expressed in terms of the nodal coordinates of the two adjoining facets. Using the vectors $\mathbf{a}$, $\mathbf{b}$ and $\mathbf{c}$, the following expression holds: $\sin(\theta) = \frac{1}{\sin(\gamma)\sin(\beta)} \frac{1}{|\mathbf{a}|^3|\mathbf{b}||\mathbf{c}|} (\mathbf{a} \times (\mathbf{c} \times \mathbf{a})) \cdot (\mathbf{a} \times \mathbf{b})$. Here γ is the angle between $\mathbf{a}$ and $\mathbf{b}$, and β the angle between $\mathbf{a}$ and $\mathbf{c}$.

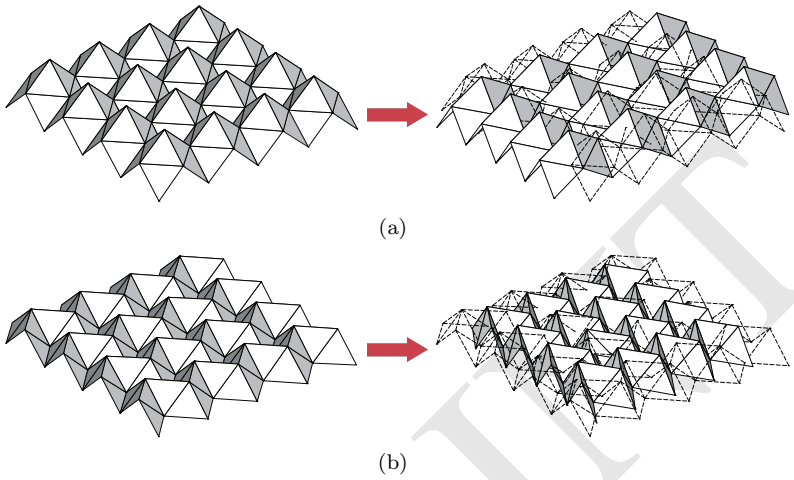

Figure 6: The Eggbox (a) and Miura (b) sheet both exhibit a single planar mechanism when the facets are not allowed to bend, as described in Section 3.2. The reference configuration is indicated as dashed lines.

stretching of the facets is allowed. In order to track the motion of the folded sheet, one iteratively follows the infinitesimal mechanisms whilst correcting for the errors using the Moore-Penrose pseudo-inverse [see, *e.g.* Tachi 06]. Our interest, however, remains with the first-order infinitesimal displacements.

In the case of the two example textured sheets, the kinematic analysis provides a single degree of freedom planar mechanism; see Figure 6. In this mechanism the facets neither stretch nor bend. This is the mechanism a rigid origami simulator would find.

3.3 Stiffness Analysis

A kinematic analysis of a framework, even with additional constraints, can clearly only provide so much information. The next step is to move from a purely kinematic to a stiffness formulation. Equations 1–3 can be combined into a single equation, relating external applied forces $\mathbf{f}$ to nodal displacements $\mathbf{d}$ by means of the material stiffness matrix $\mathbf{K}$.

$$\mathbf{K}\mathbf{d} = \mathbf{f} \tag{7}$$

$$\mathbf{K} = \mathbf{A}\mathbf{G}\mathbf{C} = \mathbf{C}^T\mathbf{G}\mathbf{C} \tag{8}$$

What is not immediately obvious is that this can easily be extended to other sets of constraints by extending the compatibility matrix.

$$\mathbf{K} = \begin{bmatrix} \mathbf{C} \\ \mathbf{J} \end{bmatrix}^T \begin{bmatrix} \mathbf{G} & 0 \\ 0 & \mathbf{G}_J \end{bmatrix} \begin{bmatrix} \mathbf{C} \\ \mathbf{J} \end{bmatrix} \tag{9}$$

Depending on the constraint and the resulting error that its Jacobian constitutes, either a physical stiffness value can be attributed in $\mathbf{G}_J$ or a 'weighted stiffness' indicating the relative importance of the constraint. In our case, the error is the change in the dihedral angle between adjacent facets. In effect, we introduce a bending stiffness along the fold line (K_{fold}) and across the facets (K_{facet}) — see Figure 4. As a result, we obtain a material stiffness matrix that incorporates the stiffness of the bars, as well as the bending stiffness of the facets and along the fold lines.

Plotting the mode shapes for the lowest eigenvalues of the material stiffness matrix $\mathbf{K}$ provides insight into the deformation kinematics of the sheets. Of main interest are the deformation modes that involve no bar elongations (*i.e.*, no stretching of the material), but only bending of the facets and along fold lines. These modes are numerically separated by choosing the axial members stiffness of the bars to be several orders of magnitude larger than the bending stiffness for the facets and folds. In our analysis only first-order infinitesimal modes within $\mathbf{K}$ are considered.

An important parameter in the folded textured sheets turns out to be $K_{\text{ratio}} = K_{\text{facet}}/K_{\text{fold}}$. This is a dimensionless parameter that represents the material properties of the sheet. When $K_{\text{ratio}} \to \infty$ we approach a situation where rigid panels are connected by frictionless hinges; values of $K_{\text{ratio}} \approx 1$ reflect folded sheets manufactured from sheet materials such as metal, plastic and paper; and when $K_{\text{ratio}} < 1$ the fold lines are stiffer than the panels, which is the case for work-hardened metals or situations where separate panels are joined together, for example by means of welding.

The results for the Eggbox and Miura sheet are shown in Figure 7 and Figure 8 respectively. The graphs show a log-log plot of the eigenvalues versus the stiffness ratio $K_{\text{facet}}/K_{\text{fold}}$. It can be seen that the salient kinematics (the softest eigenmodes) remain dominant over a large range of the stiffness ratio; this indicates that the dominant behaviour is dependent on the geometry, rather than the exact material properties. The eigenvalues can straightforwardly be plotted in terms of a combination of different parameters, such as the fold depth and different unit cell geometries, to obtain further insight into the sheets.

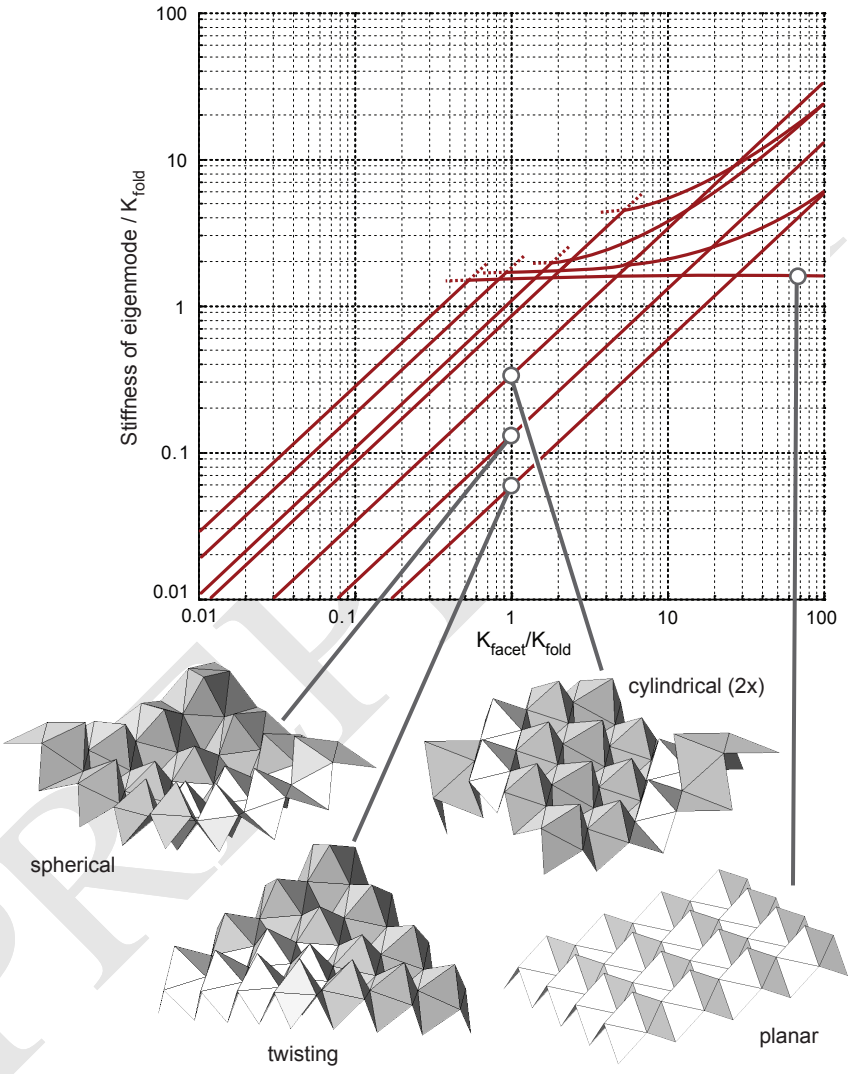

Figure 7: Here is plotted the relative stiffness of the nine softest eigenmodes of the Eggbox sheet. It can be seen that the twisting deformation mode remains the softest eigenmode over a large range of K_{ratio}. The spherical and cylindrical deformation modes observed in the models are also dominant. As $K_{\text{ratio}} \to \infty$ the planar mechanism becomes the softest eigenmode; this corresponds with the result from the kinematic analysis.

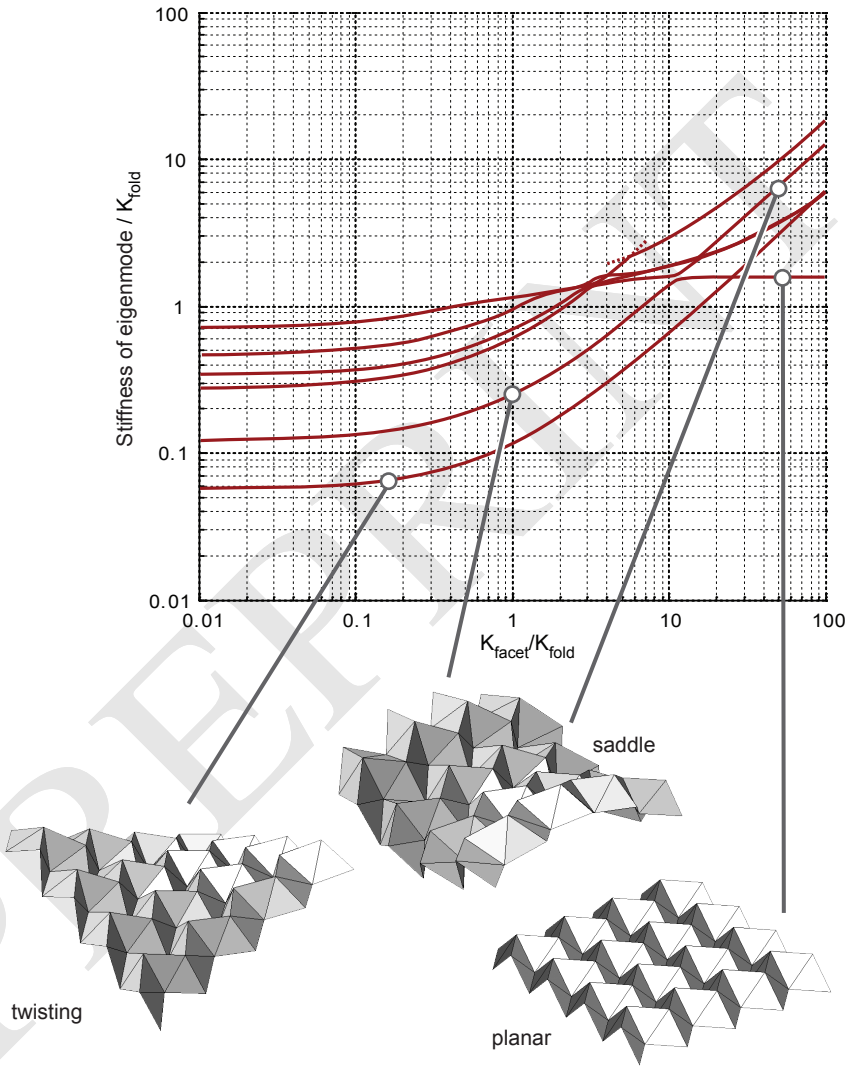

Figure 8: This figure shows the relative stiffness of the six softest eigenmodes of the Miura sheet. The twisting deformation mode remains the softest eigenmode over a large range of K_{ratio}, while the saddle-shaped mode is also dominant. As $K_{\text{ratio}} \to \infty$ the planar mechanism identified in the kinematic analysis becomes the softest eigenmode.

3.4 Coordinate Transformation

Currently all properties of the folded sheet are expressed in terms of the displacements of the nodal coordinates. The use of the (change in) fold angles may be more intuitive to Origamists, and can improve understanding of the modes. This can be done using a coordinate transformation. The transformation matrix $\mathbf{T}$ converts nodal displacements $\mathbf{d}$ to changes in angle $d\theta$:

$$d\theta = \mathbf{T}\mathbf{d} \tag{10}$$

where $\mathbf{T}$ is identical to the Jacobian in Equation 5.

4 Conclusion

This paper has presented the idea of Folded Textured Sheets, where thin-walled sheets are textured using a fold pattern, inspired by Origami folding. When considering the resulting sheets as a plate or shell, the two example sheets exhibit several remarkable properties: they can undergo large changes in shape and can alter their global Gaussian curvature by virtue of the folds opening and closing; they also exhibit unique behaviour where the apparent Poisson's ratio is oppositely signed in bending and extension.

The proposed modelling method, which represents the partially folded sheet as a pin-jointed bar framework, enables a nice transition from a purely kinematic to a stiffness matrix approach, and provides insight into the salient behaviour without the expense of a full Finite Element analysis. It captures the important behaviour of the two example sheets, and indicates that the dominant mechanics are a result of the geometry rather than the exact material properties.

References

[Alderson et al. 10] A. Alderson, K.L. Alderson, G. Chirima, N. Ravirala, and K.M. Zied. "The in-plane linear elastic constants and out-of-plane bending of 3-coordinated ligament and cylinder-ligament honeycombs." *Composites Science and Technology* 70:7 (2010), 1034–1041.

[Balkcom 04] Devin J. Balkcom. "Robotic origami folding." Ph.D. thesis, Carnegie Mellon University, 2004.

[Basily and Elsayed 04] B. Basily and E.A. Elsayed. "Dynamic axial crushing of multilayer core structures of folded Chevron patterns." *International Journal of Materials and Product Technology* 21:1–3 (2004), 169–185.

[Engel 68] Heino Engel. *Structure Systems*. Praeger, 1968.

[Guest and Pellegrino 92] S. D. Guest and S. Pellegrino. "Inextensional Wrapping of Flat Membranes." In *First International Conference on Structural Morphology*, edited by R. Motro and T. Wester, pp. 203–215. Montpellier, 1992.

[Heimbs et al. 07] S. Heimbs, P. Middendorf, S. Kilchert, A. F. Johnson, and M. Maier. "Experimental and Numerical Analysis of Composite Folded Sandwich Core Structures Under Compression." *Journal Applied Composite Materials* 14:5-6 (2007), 363–377.

[Huffman 76] D. A. Huffman. "Curvatures and Creases: A Primer on Paper." *IEEE Transactions on Computers* C-25:10 (1976), 1010–1019.

[Kuribayashi et al. 06] Kaori Kuribayashi, Koichi Tsuchiya, Zhong You, Dacian Tomus, Minoru Umemoto, Takahiro Ito, and Masahiro Sasaki. "Self-deployable origami stent grafts as a biomedical application of Ni-rich TiNi shape memory alloy foil." *Materials Science and Engineering: A* 419:1-2 (2006), 131–137.

[Lakes 87] R. Lakes. "Foam Structures with a Negative Poisson's Ratio." *Science* 235:4792 (1987), 1038 – 1040.

[Lim 07] Teik-Cheng Lim. "On simultaneous positive and negative Poisson's ratio laminates." *Physica Status Solidi (b) Solid State Physics* 244:3 (2007), 910 – 918.

[Pellegrino and Calladine 86] S. Pellegrino and C. R. Calladine. "Matrix analysis of statically and kinematically indeterminate frameworks." *International Journal of Solids and Structures* 22:4 (1986), 409–428.

[Tachi 06] Tomohiro Tachi. "Simulation of Rigid Origami." In *Proceedings of The Fourth International Conference on Origami in Science, Mathematics, and Education (4OSME)*. California Institute of Technology, Pasadena, California, USA, 2006.

[Temmerman 07] Niels De Temmerman. "Design and Analysis of Deployable Bar Structures for Mobile Architectural Applications." Ph.D. thesis, Vrije Universiteit Brussel, 2007.

[Thill et al. 08] C. Thill, J. Etches, I. Bond, K. Potter, and P. Weaver. "Morphing skins - A review." *The Aeronautical Journal* 112:1129 (2008), 117–138.

[Watanabe and Kawaguchi 06] Naohiko Watanabe and Ken'ichi Kawaguchi. "The Method for Judging Rigid Foldability." In *Proceedings of The Fourth International Conference on Origami in Science, Mathematics, and Education (4OSME)*, edited by R. Lang. California Institute of Technology, Pasadena, California, USA., 2006.

[Weina and You 10] Wu Weina and Zhong You. "Energy absorption of thin-walled tubes with origami patterns." In *5th International Conference on Origami in Science, Mathematics and Education.* Singapore, 2010.